This article has been accepted for publication in a future issue of this journal, but has not been fully edited. Content may change prior to final publication. Citation information: DOI 10.1109/TIE.2018.2868274, IEEE Transactions on Industrial Electronics

A Novel Stick-Slip Piezoelectric Actuator Based on a Triangular Compliant Driving Mechanism

Yangkun Zhang, Yuxin Peng, Zhenxing Sun, *Member*, *IEEE* and Haoyong Yu, *Member, IEEE*

***Abstract*—There are increasing demands for positioning actuators with higher resolution, accuracy, speed, and driving force. Various piezoelectric actuators have been proposed to meet these requirements. However, they all have inherent limitations. This paper presents a novel high performance piezoelectric actuator that can overcome the limitations of the existing designs. It is based on stick-slip actuation principle and makes use of coupling motions of the proposed triangular driving mechanism to generate a clamping action during the 'stick' phase and a releasing action during the 'slip' phase. Unlike existing driving mechanisms based on similar principle, the proposed one can employ its unique structure to amplify the clamping force and the related driving force by using a large design triangular angle. Besides its superior performance in driving force, it is interestingly found that, when the design angle is increased, the driving speed performance is also improved simultaneously. Finite element analysis and experiments are carried out to justify the superior performance of the proposed actuator. In comparisons with existing actuator prototypes based on similar principle, even driven with a lower input voltage, a porotype of the proposed actuator achieves a 11 times larger driving load and a 3 times higher free-load driving speed.**

***Index Terms*—Stick-slip actuator, piezoelectric, complaint mechanism, large driving force, large working stroke**

I. INTRODUCTION

HIGH-PRECISION positioning technologies play critical roles in many industrial and scientific fields, such as ultra-precision machining [1], biomedical manipulations [2]-[4], and optical systems [5]. With the fast development of these fields, there are increasingly high functional requirements for positioning actuators such as high resolution and accuracy, long stroke, high speed and large driving force [6], [7].

Although being capable of fast speed, long stroke and large output force, traditional positioning actuators like ball screws are hard to meet the demand for increasingly high accuracy in micro/nano-manipulation due to their low resolution and other problems [8]-[10]. To meet the demand for high resolution and accuracy, piezoelectric materials, which can be combined with current control strategy [11]-[15] to achieve nano-meter level resolution and accuracy, have attracted extensive attentions and various types of piezoelectric actuators, including direct-push type, ultrasonic type, inchworm type and stick-slip type have been developed in recent years. Direct-push type can achieve fast speed and large force but is limited by stroke [16]-[19]. Without stroke limit, ultrasonic-type can achieve a high driving speed [20] but suffers from low driving force, wear and heat generation problem [7]. Inchworm type is also free from stroke limit with a large driving force but the operation process is complex as it involves at least 3 independent controls to implement a series of clamping, feeding and releasing motions. As a result, the driving frequency and speed of inchworm type actuators is limited [10] , [21], [22]. Stick-slip type has a simple operation and structure [23], [24], and can combine with the dual-servo control method [25] to achieve long stroke as well as high accuracy but it has limited driving force. Those conventional types of piezoelectric actuators all have their corresponding drawbacks. To overcome all the limitations, new types of piezoelectric actuators need to be developed.

Recently, a new type of stick-slip piezoelectric actuator with clamping-releasing actions was proposed [7], [25]-[27] to address the driving force limitation of conventional stick-slip piezoelectric actuators. As shown in Fig. 1, the basic idea is to employ coupling motions at the driving point to generate a clamping action during the 'stick' phase and a releasing action during the 'slip' phase. To achieve the required coupling motions, various driving mechanisms, including parallelogram-type [26], bridge-type [25], trapezoid-type [27] and 'Z' type [7], were proposed. However, those driving mechanisms all have an inherent limit in improving the driving force of stick-slip actuators. As illustrated in Fig.1, in existing driving topologies

Manuscript received December 17, 2017; revised April 21, 2018 and July 12, 2018 respectively; accepted August 19, 2018. This work was supported in part by Temasek Laboratory at NUS, National University of Singapore and in part by the Jiangsu Province Natural Science Foundation of China (Grant No. BK20160374). *(Corresponding author: Haoyong Yu.)*

Y. Zhang and H. Yu are with the Department of Biomedical Engineering, National University of Singapore, 117576 Singapore (e-mail: zyk.engineering@gmail.com; bieyhy@nus.edu.sg).

Y. Peng is with the Department of Physical Education and Sports Science, Zhejiang University, Hangzhou 310028, China (e-mail: yxpeng@zju.edu.cn).

Z. Sun is with the Department of Electrical Engineering and Control Science, Nanjing Tech University, Nanjing 211816, China (e-mail: snzhenxing@hotmail.com).

0278-0046 (c) 2018 IEEE. Personal use is permitted, but republication/redistribution requires IEEE permission. See http://www.ieee.org/publications_standards/publications/rights/index.html for more information.

This article has been accepted for publication in a future issue of this journal, but has not been fully edited. Content may change prior to final publication. Citation information: DOI 10.1109/TIE.2018.2868274, IEEE Transactions on Industrial Electronics

[7], [25]-[27], no matter how their design parameters are changed, the clamping force $F_{clamping}$ cannot exceed the input piezo force F_{piezo} ($F_{clamping} \leq F_{piezo}$ for any α), thus limiting the driving force performance.

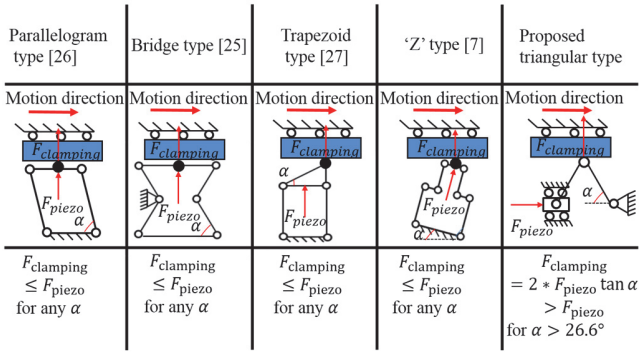

Fig. 1. Existing and proposed driving topologies of stick-slip piezoelectric actuator with clamping-releasing actions

To overcome the limitation, we developed a novel stick-slip actuator based on a triangular compliant driving mechanism. The proposed triangular driving mechanism has the following superiorities over existing driving mechanisms:1) As illustrated in Fig. 1, unlike existing driving topologies where the output clamping force is limited ($F_{clamping} \leq F_{piezo}$ for any α), the proposed one can employ its structure (by using a large α, $F_{clamping} > F_{piezo}$ when $\alpha > 26.6°$) to amplify the clamping force and the related driving force. 2) Besides, it is interestingly found that, in the proposed driving topology, for equivalent input piezo force, when the design angle α is increased for a large driving force, the feeding displacement $l_{feeding}$ is also increased, thus also enabling a superior performance in driving speed.

The rest of the paper is structured as follows. Section II introduces the configuration and operation principle of the proposed actuator. In Section III, the proposed driving mechanism is analyzed in conjunction with finite element (FE) simulations to justify its inherent superiority of amplifying the driving force by using a large design triangular angle and meanwhile investigate other effects of increasing the design angle. In Section IV, a prototype was built and a series of experiments were carried out to investigate its performance and experimentally validate the superiorities of the proposed triangular driving mechanism over existing driving mechanisms. The dynamics and control of the proposed actuator is briefly discussed in Section V and the paper is concluded in Section VI.

II. Configuration And Operation Principle

In this section, the configuration and the operation principle of the proposed actuator are introduced.

A. Configuration

As shown in Fig. 2, the actuator is composed of a base, a preload mechanism, a piezo-stack, the proposed triangular compliant driving mechanism and a slider. The piezo-stack is installed into the groove of the driving mechanism by a bolt and the driving mechanism is preloaded to the slider by a preload mechanism, which can move along the y direction to adjust the contact force between the driving mechanism and the slider. The detailed structure of the proposed triangular compliant driving mechanism and its simplified motion model are shown in Fig. 3 and Fig. 4 respectively. The driving mechanism consists of one piezo-stack installing groove, a set of fixing holes, a set of linear-motion guiding flexure hinges, and a driving foot composed of two rigid links and three rotational flexure hinges. As shown in Fig. 4, when the piezo-stack pushes the driving mechanism, it generates the required coupling motions at the driving point '0', providing clamping and releasing action and meanwhile feeding action on the slider.

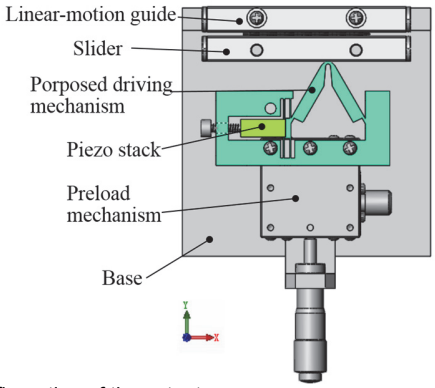

Fig. 2. Configuration of the actuator

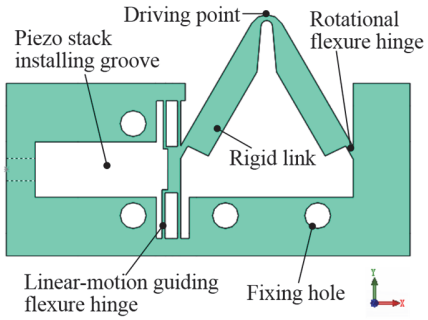

Fig. 3. Structural model of the triangular compliant driving mechanism

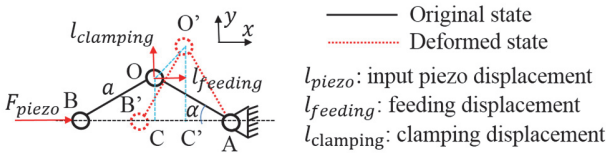

Fig. 4. Motion model of the triangular compliant mechanism

B. Operation principle

The operation principle is shown in Fig. 5. Note, in Fig. 5, the micrometer-scale deformation of the piezo is exaggerated to better illustrate the working principle of the proposed actuator. A sawtooth waveform voltage (a slow increase and a rapid decrease) is applied to drive the actuator and the complete operation cycle of the proposed actuator involves the following process.

0278-0046 (c) 2018 IEEE. Personal use is permitted, but republication/redistribution requires IEEE permission. See http://www.ieee.org/publications_standards/publications/rights/index.html for more information.

This article has been accepted for publication in a future issue of this journal, but has not been fully edited. Content may change prior to final publication. Citation information: DOI 10.1109/TIE.2018.2868274, IEEE Transactions on Industrial Electronics

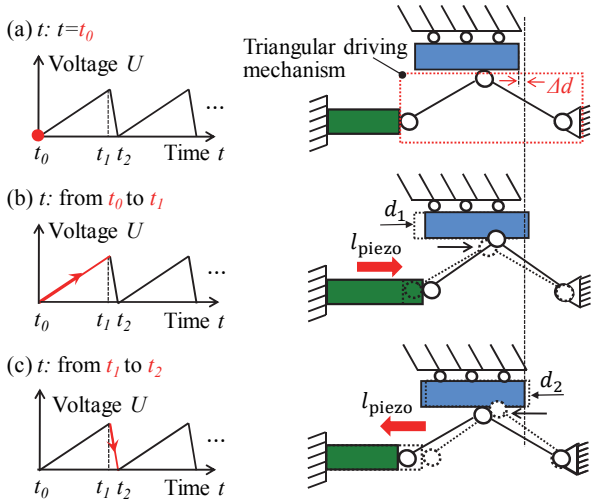

Fig. 5. Operation process of the actuator (a) Initial state; (b) the piezo-stack expands slowly; (c) the piezo-stack contracts rapidly.

Initially, at time t_0 as shown in Fig. 5 (a), with no voltage applied, the piezo-stack is at its original state and there is a contact force between the driving mechanism and the slider provided by pre-adjusting the preload mechanism.

From t_0 to t_1 as shown in Fig. 5 (b), with the slow increase of the voltage, the piezo-stack expands also slowly to push the triangular driving mechanism. When the driving mechanism is pushed along the x direction, it will induce coupling motions at driving point, clamping the slider and meanwhile moving it forward by friction force over a distance d_1.

From t_1 to t_2 as shown in Fig. 5 (c), with the rapid decrease of the voltage, the piezo-stack contracts also rapidly to its initial state. During the contraction of the piezo-stack, the driving mechanism will release the slider and move backward quickly. Due to the releasing action of the driving mechanism and the inertia of the slider, the slider would remain nearly on site (here it is assumed to be moved by d_2). Note, d_2 could be positive, negative or zero, depending on the driving frequency and amplitude of the sawtooth waveform voltage as well as other conditions such as the preload force and loading forces.

The process above completes one operation cycle of the actuator, which results in a net displacement Δd of the slider ($\Delta d = d_1 - d_2$). By repeating the process, the actuator can provide a long range linear motion step by step.

It can be noted that the principle of the actuator is similar to that of stick-slip actuators. However, unlike conventional ones whose contact force is fixed during the operation, the actuator employs the coupling motions of the triangular driving mechanism to generate a clamping action during the 'stick' phase and a releasing action during the 'slip' phase, which can effectively improve the driving force. The unique features and the related superiorities of the proposed triangular driving mechanism over existing driving mechanisms based on similar principle are justified in the following section.

III. Analysis Of The Proposed Triangular Compliant Driving Mechanism

In this section, the proposed driving mechanism is analyzed in conjunction with finite element (FE) simulations to justify its inherent superiority of amplifying the driving force by using a large design triangular angle and meanwhile investigate other effects of increasing the design angle.

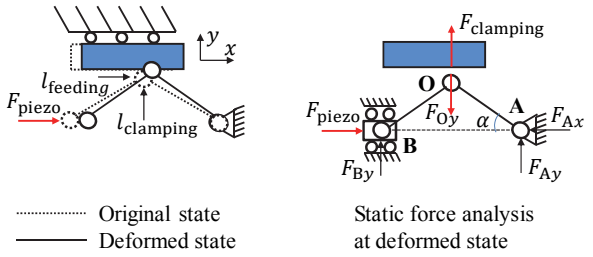

Fig. 6. Force analysis

The simplified analytical model was first used to justify the unique features and the related superiorities of the proposed triangular driving mechanism. Considering the static deformed state with reference to Fig. 6 and taking the translational joint and three revolute joints in the proposed triangular driving topology as ideal ones, the following relations can be derived from the force balance along x and y directions and the moment balance of OB and OA:

$$F_{Ax} = F_{piezo}, \tag{1}$$

$$F_{clamping} = F_{Oy} = F_{piezo} \tan\alpha + F_{Ax} \tan\alpha = 2F_{piezo} \tan\alpha. \tag{2}$$

In (1) and (2), F_{Ax} is the support force from the base along x direction at flexure A and F_{Oy} is the reaction force from the slider along y direction at driving point O.

It can be easily seen from (2) that, unlike existing driving topologies where the output clamping force is limited ($F_{clamping} \leq F_{piezo}$) shown in Fig.1, the proposed driving topology can employ its structure (by using a large design angle α and $F_{clamping} > F_{piezo}$ when $\alpha > 26.6°$) to amplify the clamping force and the related driving force. Note, the amplification of the output clamping force is with regard to the input piezo force F_{piezo}.

To further verify this unique feature of the proposed driving mechanism that the clamping force can be amplified by using a large design angle α, the clamping force $F_{clamping}$ of the proposed triangular driving mechanism with α=30°, 45°, 60° under the same input force and boundary conditions are respectively simulated by using the finite element method (FEM).

Finite element models are created in the commercial software ANSYS and the models are auto meshed with the contacts and flexure hinges refined as shown in Fig.7. In the simulations, the driving mechanism and the linear-mode guide for the slider are fixed accordingly. The contact condition between the slider and the linear-motion guide for the slider is defined as 'no separation', which allows frictionless translation of the slider with no separation between the slider and the guide in the tangential direction. The contact condition between the driving foot and the slider is defined as 'frictional' with the friction coefficient defined as 0.2. 65Mn (the density, elastic modulus,

0278-0046 (c) 2018 IEEE. Personal use is permitted, but republication/redistribution requires IEEE permission. See http://www.ieee.org/publications_standards/publications/rights/index.html for more information.

This article has been accepted for publication in a future issue of this journal, but has not been fully edited. Content may change prior to final publication. Citation information: DOI 10.1109/TIE.2018.2868274, IEEE Transactions on Industrial Electronics

and Poisson ratio are respectively set as 7810 kg/m3, 226 GPa and 0.3) is set as material of the driving mechanism and structural steel (the density, elastic modulus, and Poisson ratio are respectively set as 7850 kg/m3, 200 GPa and 0.3) is set as the material of the slider and the guide. The input piezo force F_{piezo} is set as 1000N and applied on the surface where the piezo stack is located.

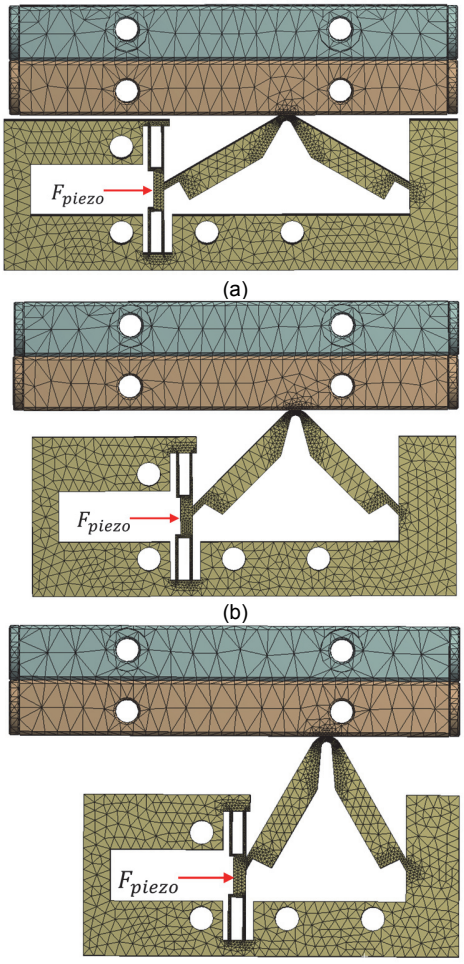

Fig. 7. Meshed finite element models (a) α=30° ; (b) α=45° ; (c) α=60°

TABLE I
SIMULATION RESULTS

		$\alpha = 30°$	$\alpha = 45°$	$\alpha = 60°$
Clamping force $F_{clamping}$ (N)	Equation (2)	1155	2000	3464
	FEM	1054	1758	2636
Feeding displacement $l_{feeding}$ (μm)	FEM	14	22	43
Maximum structural stress σ_{max} (GPa)	FEM	0.65	1.12	1.69

The clamping force is simulated by using 'force reaction' in 'contact tool' of ANSYS workbench. The FE simulation results together with those calculated by (2) are summarized in Table I. Both results validate the superiority of the proposed driving topology that it can employ its structure (by using a large design angle α) to amplify the clamping force (note, the amplification of the clamping force is with regard to the input force which is 1000N). The results simulated by FEM are less than those calculated by (2). This is because flexure hinges have certain stiffness in guiding linear or rotational motion and therefore reduce the force output.

To investigate other effects of increasing design angle α, the feeding displacement and the structural stress are also simulated by FEM. The directional deformation results of different design angle α in motional direction (Y axis in this case) are shown in Fig.8 with the feeding displacement simulation results summarized in Table I. It can be seen that for equivalent input force, the feeding displacement also increases with the rise of the design angle α, which means for equivalent driving frequency f (limited by the actuator bandwidth), the driving speed v can be increased, since $v \approx f l_{feeding}$. Therefore, by increasing the design angle α, it can not only improve the driving force performance but also the driving speed performance.

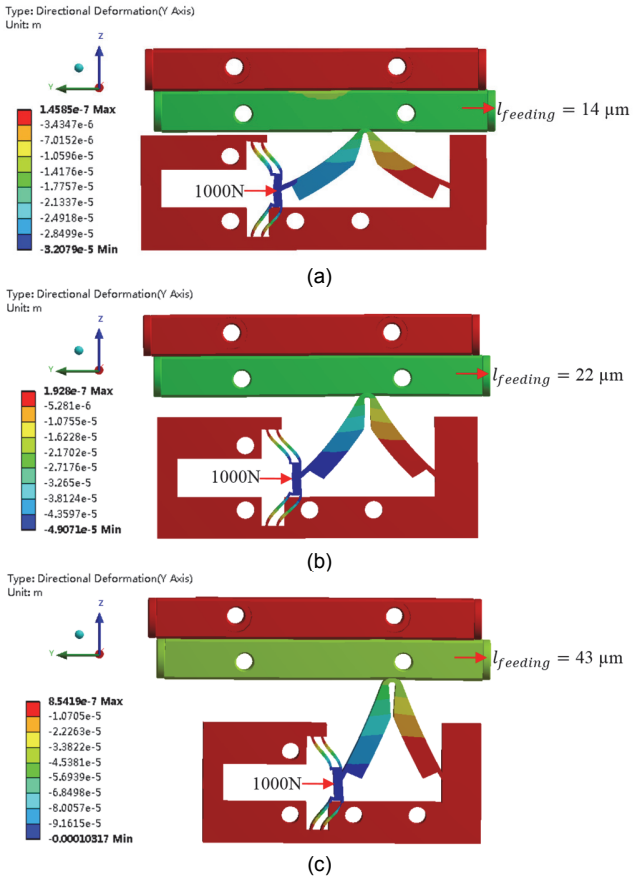

Fig. 8. Deformation in moving direction (a) α=30° ; (b) α=45° ; (c) α=60°

In terms of structure stress, the related Von-Mises stress distribution are shown in Fig. 9 with the maximum structural stress σ_{max} summarized in Table I. The simulation results show that the structural stress rises with the increase of design angle α. This is expected, since when the clamping force the slider receives from the driving mechanism increases, the related reaction force the driving mechanism receives from the slider will also increase. Therefore, when the design angle is increased to improve the performance, a special care needs to be taken to ensure that the structural stress is within an allowable range in

0278-0046 (c) 2018 IEEE. Personal use is permitted, but republication/redistribution requires IEEE permission. See http://www.ieee.org/publications_standards/publications/rights/index.html for more information.

This article has been accepted for publication in a future issue of this journal, but has not been fully edited. Content may change prior to final publication. Citation information: DOI 10.1109/TIE.2018.2868274, IEEE Transactions on Industrial Electronics

case of mechanical failure of material and structure.

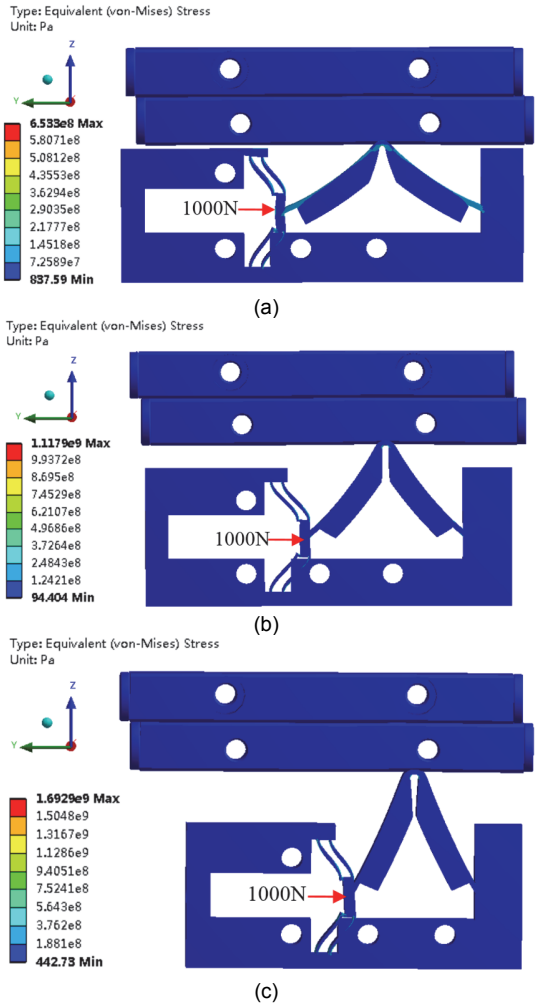

Fig. 9. Von-Mises stress distribution (a) α=30° ; (b) α=45° ; (c) α=60°

IV. EXPERIMENTS

In this section, a prototype of the proposed actuator was built and a series of experiments were carried out to investigate its performance and experimentally validate its aforementioned superiorities.

A. Prototype and experimental set-up

With reference to Fig. 10 (a), a prototype of the proposed actuator was built. A large design angle $\alpha = 60°$ with $a = 20$ mm is chosen to achieve large driving force and high driving speed and 65Mn is selected as the design material for its good elastic properties. The proposed triangular compliant driving mechanism was fabricated in a monolithic structure via wire-cut electrical discharge machining (WEDM). The piezo-stack used for driving is SA070718 from Piezo Drive with a size of 7mm×7mm×18mm. For the slider, a cross-roller linear guide from THK (VR4-80HX7Z) is selected due to its high stiffness and compact size and the working stroke of the slider is 30 mm. A manual X axis stage from Optics Focus (MAX-P40C-13) is used as the preload mechanism. The overall dimension of the prototype is 140 mm×100 mm×37 mm.

The experimental set-up was established as shown in Fig. 10 (a) with the experimental schematic shown in Fig. 10 (b). A function generator (33220A from KEYSIGHT) is used to generate the required sawtooth waveform voltage signals. The signals are amplified by a voltage amplifier (ENP-151U from ECHO ELECTRONICS) to drive the actuator. The output motion of the slider is measured by a laser sensor (LK-H052 from KEYENCE) and the data are recorded by an oscilloscope (DLM2024 from YOKOGAWA). Besides, a standard string-pulley-weight system is added into the experimental setup to investigate the force loading capacity of the actuator. The self-locking force of the actuator, the largest load that the slider can hold without inputting any voltage to the piezo-stack, was pre-adjusted by the preload mechanism to be around 60N and no further adjustment is applied during all the experiments.

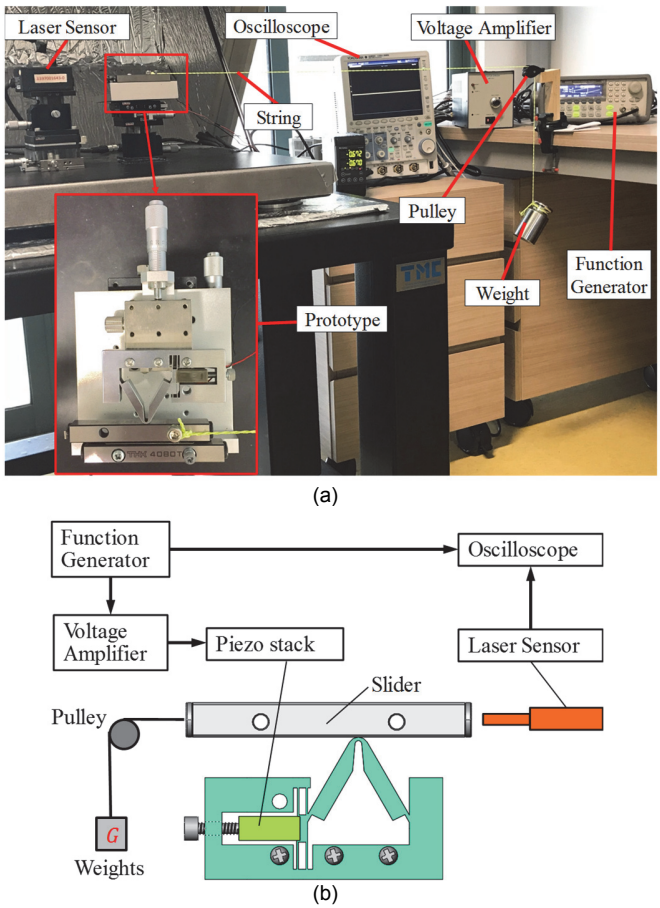

Fig. 10. Experimental system (a) setup and prototype; (b) schematic

B. Experiments and discussions

The relation between driving frequency f and output velocity v of the slider was first investigated to identify the optimal working frequency of the actuator. The driving voltage was kept the same as 80 Vp-p. As shown in Fig. 11, with the rise of the driving frequency, the output velocity of the slider first increased and reached a peak at 3500 Hz and, after that, it began to decrease. This increasing trend of output velocity v with the frequency f could be easily understood, since the output velocity can be expressed as $v = f \cdot \Delta d$. However, as every actuator has limited bandwidth, when the operation

0278-0046 (c) 2018 IEEE. Personal use is permitted, but republication/redistribution requires IEEE permission. See http://www.ieee.org/publications_standards/publications/rights/index.html for more information.

This article has been accepted for publication in a future issue of this journal, but has not been fully edited. Content may change prior to final publication. Citation information: DOI 10.1109/TIE.2018.2868274, IEEE Transactions on Industrial Electronics

frequency is beyond the bandwidth, the displacement output magnitude of the driving mechanism will dramatically decrease with the increase of the frequency, resulting in a decreasing output step displacement of the slider Δd. Although the frequency increases, as the step displacement Δd decreases in a faster rate, the output velocity then showed a decreasing trend. Therefore, the optimal driving frequency for the actuator, which corresponds to a high mechanical power, was found to be 3500 Hz. This optimal frequency would be used as the driving frequency for the rest of the experiments.

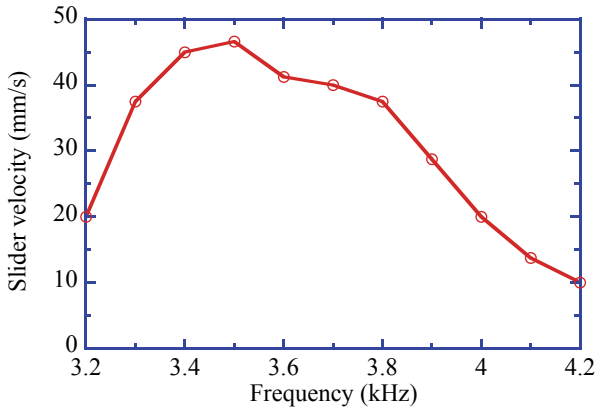

Fig. 11. Relation between driving frequency and output slider velocity

Then, the relation between driving voltage and output velocity v of the slider was investigated. The driving frequency f is fixed at 3500 Hz and the experimental data were plotted in Fig. 12. The starting voltage for stably driving the slider was found to be 13 V, which corresponds to a velocity v around 0.14 mm/s and a step displacement Δd around 40 nm with reference to Fig. 13. Therefore, the actuator can achieve a positioning resolution of 40nm. When the voltage is above 13 V, it can be seen from Fig. 12 that the output velocity goes almost linearly with the increase of the voltage, which means the slider velocity (and the step displacement Δd, since $\Delta d = v/f$ and the driving frequency f is fixed) can be linearly controlled by the driving voltage. With reference to Fig. 14, the proposed actuator achieved an output velocity of 46.67 mm/s under the driving voltage of 80 V. The driving speed can be further improved by increasing the driving voltage. However, the voltage amplifier used in this experiment is not powerful enough to drive the actuator above 80 V at 3500 Hz.

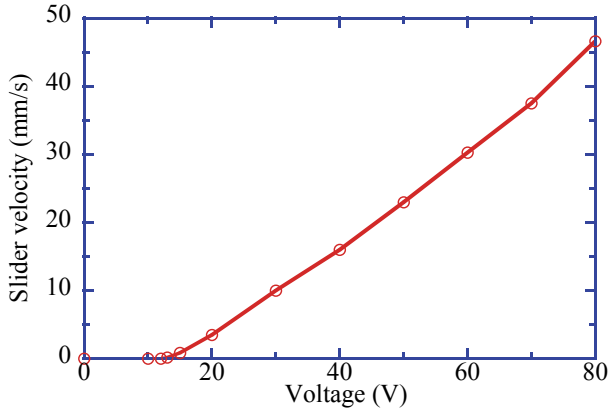

Fig. 12. Relation between driving voltage and output slider velocity

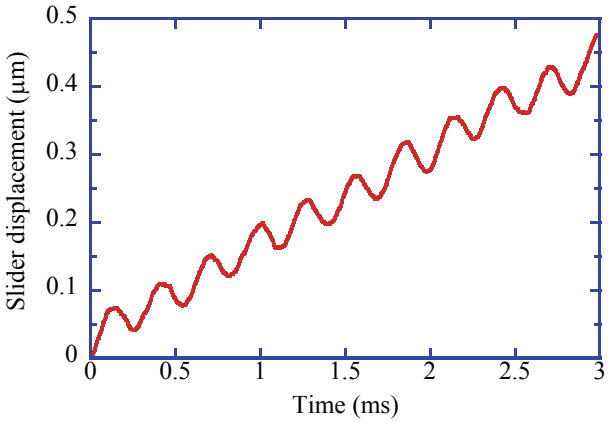

Fig. 13. Slider motion under the applied voltage of 13 V

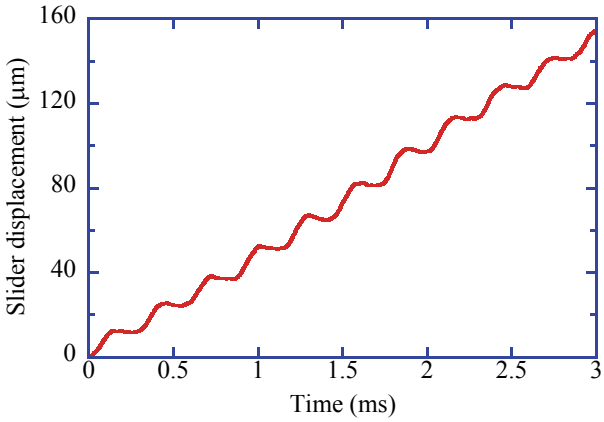

Fig. 14. Slider motion under the driving voltage of 80 V

After that, the string-pulley-weight system was used to test the force loading capacity of the actuator in the driving direction, as shown in Fig. 9. The driving frequency and voltage are fixed at 3500 Hz and 80 V respectively, and, by varying standard weights, output velocities of the slider were measured by laser sensor and were plotted in Fig. 15. It can be seen that the slider velocity almost linearly decreases with the increase of the loads. With reference to Fig. 16, even under the load of 4 kg applied in the driving direction, the actuator can still drive the slider stably with a velocity of 0.7 mm/s.

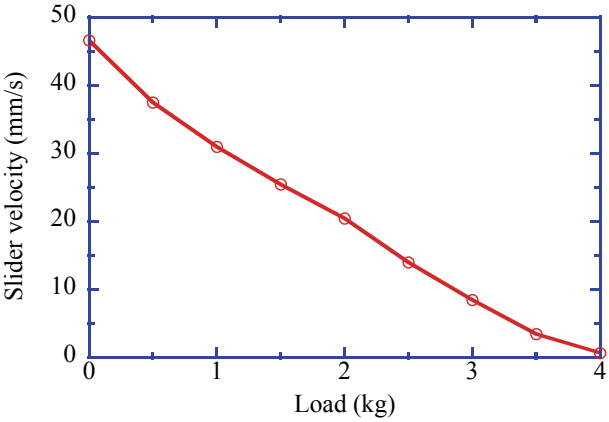

Fig. 15. Force-loading capacity in the driving direction

0278-0046 (c) 2018 IEEE. Personal use is permitted, but republication/redistribution requires IEEE permission. See http://www.ieee.org/publications_standards/publications/rights/index.html for more information.

This article has been accepted for publication in a future issue of this journal, but has not been fully edited. Content may change prior to final publication. Citation information: DOI 10.1109/TIE.2018.2868274, IEEE Transactions on Industrial Electronics

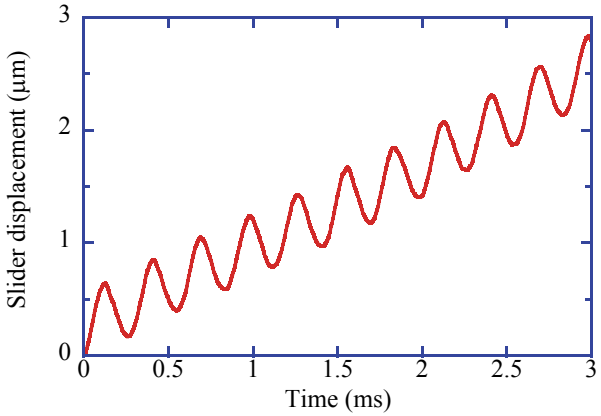

Fig. 16. Slider motion under the load of 40 N (4 kg)

C. Performance comparison with literature designs

TABLE II
PERFORMANCE COMPARISONS

Stick-slip actuators based on coupling motions of compliant driving mechanisms	Voltage (Vp-p)	Frequency (Hz)	Free-load velocity (mm/s)	Maximum Load (kg)
Parallelogram -type [26]	100	2000	14.25	0.35
Bridge-type [25]	100	1000	7.95	0.158
Trapezoid-type [27]	100	500	5.96	0.3
'Z'-type [7]	100	5000;1	6.057 (5000Hz)	0.35 (1Hz)
Proposed triangular type	80	3500	46.67	4

Table II summarizes and compares the key performance of existing compliant driving mechanisms designed for stick-slip actuators with clamping-releasing actions. In comparisons, even with a lower input voltage, the proposed driving mechanism achieves a driving load around 11 times that of the best [7], [26] of others and a free-load driving speed around 3 times that of the best [26] of others. The superior performance in the driving speed and the driving force is justified in Section III.

V. Discussions On Dynamics And Control

The main contribution of the paper is the development of a new driving topology for stick-slip actuators with clamping-releasing actions, which can achieve a considerably larger driving force and driving speed than existing driving topologies. The actuator dynamics and control are not the main focus. For the completeness, they are just briefly discussed in this section.

A simplified dynamic model of stick-slip actuators with clamping-releasing actions can be seen in [7], [25]. In the model, the driving unit composed of the piezo stack and the compliant driving mechanism is simplified as a second-order mass-spring-damper system. The contact force between the driving point and the slider is simplified as a constant and the LuGre friction model is used to model the interactions between the driving unit and the slider. In fact, the dynamics of stick-slip actuator with clamping-releasing actions are far more complex. With reference to Fig. 5, it involves the motion of the flexure-hinge based complaint driving mechanism, varying contact force induced by the clamping-releasing actions of driving mechanism and friction force involving varying contact force. However, the control of stick-slip actuators with clamping-releasing actions does not necessarily rely on modelling the complex dynamics.

Firstly, stick-slip actuators can be open-loop controlled for positioning applications via controlling the number and the voltage amplitude of input sawtooth voltage wave. However, the open-loop control strategy is not robust and the positioning accuracy is often limited.

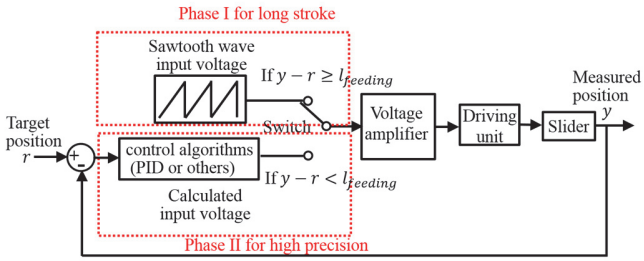

Fig. 17. Dual-loop control strategy of stick-slip actuators

As shown in Fig. 17, a dual-loop control strategy [7], [29] can be adopted to improve the positioning accuracy. It is composed of two control phases. In the first phase (coarse positioning phase), the piezoelectric actuator is electrified with a series of sawtooth voltage wave shown in Fig. 5 and the slider moves forward step by step to achieve a long stroke. When the slider is approaching the target position within the maximum feeding displacement of the driving mechanism, it comes to the second phase of control (fine positioning phase). The aim of the second phase is to achieve a high resolution and accuracy and the piezoelectric actuator is no longer electrified with sawtooth waveform voltage but with a continuously increasing voltage until the slider moves to the target position. It is shown in [7] that the stick-slip actuator can achieve a positioning accuracy as high as 10nm in the second phase of control simply by using a PID controller. To consider the inherent hysteresis from piezo [28] and the complicated relative motion between the driving mechanism and slider, a more advanced control technique [29] can be used.

VI. Conclusion

In this work, a novel stick-slip piezoelectric actuator based on a triangular compliant driving mechanism was proposed. It is based on stick-slip actuation principle and makes use of coupling motions of the proposed triangular driving mechanism to generate a clamping action during the 'stick' phase and a releasing action during the 'slip' phase, which can effectively increase the driving force. Compared with existing driving mechanisms based on similar principle, the proposed one can employ its structure to amplify the clamping force and the related driving force by using a large design triangular angle.

0278-0046 (c) 2018 IEEE. Personal use is permitted, but republication/redistribution requires IEEE permission. See http://www.ieee.org/publications_standards/publications/rights/index.html for more information.

This article has been accepted for publication in a future issue of this journal, but has not been fully edited. Content may change prior to final publication. Citation information: DOI 10.1109/TIE.2018.2868274, IEEE Transactions on Industrial Electronics

The proposed driving mechanism is analyzed in conjunction with finite element (FE) simulations to justify its superiority in driving force performance and meanwhile investigate other effects of increasing design angle. It is interestingly found that, by increasing the design angle, it can not only increase the clamping force but also increase the feeding displacement, thereby enabling superior performance in driving force and driving speed simultaneously. However, when the design angle is increased to improve the performance, a special care needs to be taken to ensure that the structural stress is within an allowable range, since the structural stress is found to rise with the increase of the design angle.

A prototype of the proposed actuator with the triangular angle designed to be 60° was built and tested. The actuator has a large powerless self-locking force of 60 N and achieves a positioning resolution of 40nm with the driving voltage of 13 V at 3500 Hz. With the driving voltage of 80 V at 3500 Hz, it achieves a free-load velocity as high as 46.67 mm/s and, even under the load of 40 N applied in the driving direction, it still achieves a stable velocity of 0.7 mm/s.

In comparisons with other designs based on similar principle, even driven with a lower input voltage, the proposed actuator achieves a driving load around 11 times larger and a free-load driving speed around 3 times higher, which validates its superior performance in both driving force and driving speed.

In future work, the proposed design will be applied in the development of a precision positioning mechanism for 3D printing applications and the structure can be optimized to further improve the performance.

REFERENCES

[1] S. Verma, W.J. Kim and H. Shakir, "Multi-axis maglev nanopositioner for precision manufacturing and manipulation applications," *IEEE Trans. Ind. Appl.*, vol. 41, no. 5, pp.1159-1167, Sep. 2005.

[2] S. Wang, H. Arellano-Santoyo, P.A. Combs and J.W. Shaevitz, "Actin-like cytoskeleton filaments contribute to cell mechanics in bacteria," *Proc. Natl. Acad. Sci. U.S.A.*, vol. 107, no. 20, pp.9182-9185, May 2010.

[3] Y. Zhang, K. K. Tan and S. Huang, "Vision-servo system for automated cell injection," *IEEE Trans. Ind. Electron.*, vol. 56, no. 1, pp. 231-238, Jan. 2009.

[4] T. Tanikawa and T. Arai, "Development of a micro-manipulation system having a two-fingered micro-hand," *IEEE T. Robot. Autom.*, vol. 15, no. 1, pp. 152-162, Aug. 2002.

[5] J.K. Fisher, J. Cribb, K.V. Desai, L. Vicci, B. Wilde, K. Keller, R.M. Taylor, J. Haase, K. Bloom, E.T. O'Brien and R. Superfine, "Thin-foil magnetic force system for high-numerical-aperture microscopy," *Rev. Sci. Instrum.*, vol. 77, no. 2, pp. 1-9 (023702), Feb. 2006.

[6] S. Wang, W. Rong, L. Wang, Z. Pei and L. Sun, "Design, analysis and experimental performance of a novel stick-slip type piezoelectric rotary actuator based on variable force couple driving," *Smart Mater. Struct.*, vol. 26, no. 5, pp. 055005, Apr. 2017.

[7] J. Li, H. Huang and H. Zhao, "A piezoelectric-driven linear actuator by means of coupling motion," *IEEE Trans. Ind. Electron.*, vol. 65, no. 5, pp. 2458-2466, Mar. 2018.

[8] J. Yang, W.H. Chen, S. Li, L. Guo, Y. Yan, "Disturbance/uncertainty estimation and attenuation techniques in PMSM drives—a survey," *IEEE Trans. Ind. Electron.*, vol. 64, no. 4, pp. 3273-3285, Apr. 2017.

[9] B. Henke, O. Sawodny and R. Neumann, "Distributed Parameter Modeling of Flexible Ball Screw Drives Using Ritz Series Discretization," *IEEE/ASME Trans. Mechatron.*, vol. 20, no. 3, pp. 1226–1235, Jun. 2015.

[10] P.E. Tenzer and R.B. Mrad, "A systematic procedure for the design of piezoelectric inchworm precision positioner," *IEEE/ASME Trans. Mechatron.*, vol. 9, no. 2, pp. 427–435, Jun. 2004.

[11] L. Cheng, W. Liu, Z. G. Hou, J. Yu and M. Tan, "Neural-network-based nonlinear model predictive control for piezoelectric actuators," *IEEE Trans. Ind. Electron.*, vol. 62, no. 12, pp. 7717-7727, Dec. 2015.

[12] X. Chen, C. Y. Su, Z. Li and F. Yang, "Design of implementable adaptive control for micro/nano positioning system driven by piezoelectric actuator," *IEEE Trans. Ind. Electron.*, vol. 63, no. 10, pp. 6471-6481, Oct.2016.

[13] Y. Cao, L. Cheng, X. B. Chen and J. Y. Peng, "An inversion-based model predictive control with an integral-of-error state variable for piezoelectric actuators," *IEEE/ASME Trans. Mechatron.*, vol. 18, no. 3, pp. 895-904, Jun. 2013.

[14] J. Y. Peng and X. B. Chen, "Integrated PID-based sliding mode state estimation and control for piezoelectric actuators," *IEEE/ASME Trans. Mechatron.*, vol. 19, no. 1, pp. 88-99, Feb. 2014.

[15] P. Ronkanen, P. Kallio, M. Vilkko and H. N. Koivo, "Displacement control of piezoelectric actuators using current and voltage," *IEEE/ASME Trans. Mechatron.*, vol. 16, no. 1, pp. 160-166, Feb. 2011.

[16] H. Tang and Y. Li, "Development and active disturbance rejection control of a compliant micro-/nanopositioning piezostage with dual mode," *IEEE Trans. Ind. Electron.*, vol. 61, no. 3, pp. 1475-1492, Mar. 2014.

[17] Q. Xu, "Design and smooth position/force switching control of a miniature gripper for automated microhandling," *IEEE Trans. Ind. Electron.*, vol. 10, no. 2, pp. 1023-1032, May 2014.

[18] Q. Xu, "Robust impedance control of a compliant microgripper for high-speed position/force regulation," *IEEE Trans. Ind. Electron.*, vol. 62, no. 2, pp. 1201-1209, Feb. 2015.

[19] F. Wang, C. Liang, Y. Tian, X. Zhao and D. Zhang, "Design and control of a compliant microgripper with a large amplification ratio for high-speed micro manipulation," *IEEE/ASME Trans. Mechatron.*, vol. 21, no. 3, pp. 1262-1271, Jun. 2016.

[20] J. Z. Shi and B. Liu, "Optimum efficiency control of traveling-wave ultrasonic motor system," *IEEE Trans. Ind. Electron.*, vol. 58, no. 10, pp. 4822-4829, Oct. 2011.

[21] S. P. Salisbury, D. F. Waechter, R. B. Mrad, and S. E Prasad, "Design considerations for complementary inchworm actuators," *IEEE/ASME Trans. Mechatron.*, vol. 11, no. 3, pp. 265-272, Jun. 2006.

[22] T. Uzunovic, E. Golubovic, and A. Sabanovic, "Piezo LEGS driving principle based on coordinate transformation," *IEEE/ASME Trans. Mechatron.*, vol. 20, no. 3, pp. 1395-1405, Jun. 2015.

[23] J. Y. Peng and X. B. Chen, "Modeling of piezoelectric-driven stick–slip actuators," *IEEE/ASME Trans. Mechatron.*, vol. 16, no. 2, pp. 394-399, Apr. 2011.

[24] M. Hunstig, T. Hemsel, and W. Sextro, "Stick-slip and slip-slip operation of piezoelectric inertia drives. Part I: Ideal excitation," *Sens. Actuators A, Phys.*, vol. 200, no. 4, pp. 90-100, Oct. 2013.

[25] J. P. Li, X. Q. Zhou, H. W. Zhao, M. K. Shao, N. Li, S. Z.Z, and Y. M. Du, "Development of a novel parasitic-type piezoelectric actuator," *IEEE/ASME Trans. Mechatron.*, vol. 22, no. 1, pp. 541-550, Feb. 2017.

[26] J. Li, X. Zhou, H. Zhao, M. Shao, P. Hou and X. Xu, "Design and experimental performances of a piezoelectric linear actuator by means of lateral motion," *Smart Mater. Struct.*, vol. 24, no. 6, pp. 065007, May 2015.

[27] T. Cheng, M. He, H. Li, X. Lu, H. Zhao and H. Gao, "A Novel Trapezoid-Type Stick–Slip Piezoelectric Linear Actuator Using Right Circular Flexure Hinge Mechanism," *IEEE Trans. Ind. Electron.*, vol. 64, no. 7, pp. 5545-5552, Jul. 2017.

[28] Z. Li and J. Shan, "Inverse compensation based synchronization control of the Piezo-actuated Fabry-Perot Spectrometer," *IEEE Trans. Ind. Electron.*, vol. 64, no.11, pp. 8588 – 8597, Jun. 2017

[29] L. Cheng, W. Liu, C. Yang, T. Huang, Z. G. Hou and M. Tan, "A Neural-Network-Based Controller for Piezoelectric-Actuated Stick–Slip Devices," IEEE *Trans. Ind. Electron.*, vol. 65, no. 3, pp. 2598-2607, Mar. 2018.

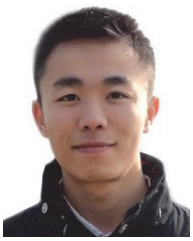

Yangkun Zhang was born in Jiangsu Province, China, in 1989. He received the Bachelor degree (1st class honor) and the Ph. D degree from the School of Mechanical Engineering, University of Adelaide, in 2012 and 2016, respectively.

He was a Visiting Ph.D Student with Nano-Metrology and Control Gao & Ito Lab, Tohoku University, Japan from 2014 to 2015 and with the lab of ultrasonic applications, Vilnius Gediminas Technical University, Lithuania, from 2015 to 2016. Since 2016, he has been with the Advanced Robotics Center,

0278-0046 (c) 2018 IEEE. Personal use is permitted, but republication/redistribution requires IEEE permission. See http://www.ieee.org/publications_standards/publications/rights/index.html for more information.

This article has been accepted for publication in a future issue of this journal, but has not been fully edited. Content may change prior to final publication. Citation information: DOI 10.1109/TIE.2018.2868274, IEEE Transactions on Industrial Electronics

National University of Singapore, as a research fellow. His research interest includes piezoelectric actuators and motors, energy harvesters, compliant mechanism, and nano-positioning technologies.

Yuxin Peng received his Bachelor and Master degrees from Chongqing University, China in 2007 and 2010, followed by PhD from the Department of Nanomechanics, Tohoku University, Japan in 2013.

He acted as a Research Fellow in the Department of Biomedical Engineering, National University of Singapore, Singapore from 2014 to 2016. He is currently a ZJU100 tenure-track professor of the Department of Physical Education and Sports Science, Zhejiang University, China. His interests include smart sensors, actuators, biomechanics, and human activity recognition.

Zhenxing Sun (M'16) received the B.Eng. degree in electrical engineering from Southeast University, Nanjing, China, in 2007. M.Eng. degree in control theory and control engineering from Nanjing Tech University, Nanjing, China, in 2012, and the Ph.D. degree in control theory and control engineering from Southeast University, Nanjing, China, in 2017.

He is currently with the Advanced Research Center, National University of Singapore, as a visiting scholar. Since December 2017, he has been Lecturer in the College of Electrical Engineering and Control Science at Nanjing Tech University, Nanjing, China. His main research interests include advanced control theory with applications to servo, robot and other mechanical systems.

Haoyong Yu (M'10) received the Ph.D. degree in Mechanical Engineering from Massachusetts Institute of Technology, Cambridge, Massachusetts, USA, in 2002.

He was a Principal Member of Technical Staff at DSO National Laboratories, Singapore, until 2002. He is currently an Associate Professor with the Department of Biomedical Engineering, National University of Singapore, Singapore. His areas of research include medical robotics, rehabilitation engineering and assistive technologies, system dynamics and control.

Dr. Yu received several best paper and poster awards at IEEE conferences. He has also served on a number of IEEE conference organizing committees.

0278-0046 (c) 2018 IEEE. Personal use is permitted, but republication/redistribution requires IEEE permission. See http://www.ieee.org/publications_standards/publications/rights/index.html for more information.